Revised version submitted to Cement and Concrete Research

Belite clinkers with increasing aluminium content: effect of calcium aluminates on calcium silicate hydration

Cinthya Redondo-Soto[1], Daniela Gastaldi[2*], Sara Irico[3], Fulvio Canonico[2], Miguel A. G. Aranda[1]*

[1] *Departamento de Química Inorgánica, Cristalografía y Mineralogía, Universidad de Málaga, 29071 Málaga, Spain*

[2] *BUILT – Buzzi Unicem Innovation Lab and Technology – Via Restano 3, 15100 Vercelli (VC), Italy*

[3] *Wilhelm Dyckerhoff Institut - Dyckerhoffstrasse 7, 65203 Wiesbaden, Germany*

** emails: dgastaldi@buzziunicem.it (D.G.), g_aranda@uma.es (M.A.G.A.)*

Abstract.

Belite cements (BCs) could have advantages over Portland cements concerning durability, low heat development and the use of less demanding raw materials. The activation of BCs by sulphur addition at the clinkering stage and by fast cooling is well established. However, the reaction rates of the calcium silicate phases, mainly belite, are still not fully understood. This is partly due to the interplay between factors including: i) belite activation during clinkering; ii) role of the calcium aluminates at early hydration ages; and iii) role of the sulphates. In the research reported here, three belite clinkers were prepared with a constant values of lime saturation factor, and SO_3, Fe_2O_3 and CaF_2 contents. The varied parameter was the amount of Al_2O_3. The resulting clinkers have overall crystalline reactive calcium aluminate contents of 0.4, 7.9 and 16.7 wt%, respectively. Cements were prepared with similar particle sizes and constant anhydrite content. Here, it is shown that calcium silicate reactivities, both alite and belite, strongly depend upon the calcium aluminate contents. As these amounts increase, the degree of hydration of alite at 1 day decreases: 85, 65 and 50 %. Furthermore, the degree of hydration of belite at 7 days was 50, 35 and 0 %. Thus, there is a strong influence of aluminates in calcium silicate rates of hydration. Moreover, comparing the mechanical properties of the cements with 0.6 and 8.2 wt% amounts of calcium aluminates, the improvements due to the higher reactivity of calcium aluminates at very early ages, seem to be counterbalanced by the lower reactivity of the silicate phases. The reported findings may allow further optimisation of early age reactivity of active BCs.

Keywords: CO_2 footprint, calcium aluminates, C-S-H gel, ettringite, Rietveld analysis, belitic cement

1. Introduction.

The seek for sustainable solutions as alternative to Portland Cement (PC) is becoming increasingly important due to the global demand of concrete, which is expected to grow by 12-23% by 2050 [1]. A critical requirement is to decrease the direct CO_2 emissions. This is difficult as two-thirds of the overall emissions are due to the decomposition of the required limestone, the other third being mainly related to energy consumption.

The reduction of the clinker factor and the use of alternative materials, both fuels and clinkers, are the three main strategies to reduce CO_2 emissions in cement manufacturing [2,3]. Some solutions are already available like calcium sulfoaluminate cements or calcium aluminate cements [4,5]. However, the raw materials needed for these cements have quite limited availabilities [6]. Hence, these binders are produced in low amounts, are expensive and used just for special applications. Limestone, clay and shale are widely available and used for Portland clinker production. An alternative clinker, included in the family of Portland clinker, are the Belite clinkers [7] which have been used for more than hundred years in applications where massive concretes were needed, i.e. dam constructions like Hoover Dam (completed in 1936) or Grand Coulee dam (completed in 1942) [8]. These belite-rich alite-poor cements are within the low heat cement category, ASTM Type IV.

Belite clinkers are characterized by a high belite and low alite contents. For the production of Portland clinker, the lime saturation factor (LSF) is generally set in the range 95-100. However, for fabricating belite clinker this value is reduced to 80-85 [9,10]. Comparing the formation of alite, equation (1), and belite, equation (2), it is evident that the production of belite releases less CO_2. The amount of CO_2 from the raw meal for the production of 1 ton of belite is 511 kg against 578 kg released by alite, i.e. a 12 % saving [2]. Moreover, the decrease of about 200°C in the kiln temperature also yields savings in the emissions from fuel consumption.

$$3\,CaCO_3 + SiO_2 \rightarrow Ca_3SiO_5 + 3CO_2 \uparrow \quad (1)$$

$$2\,CaCO_3 + SiO_2 \rightarrow Ca_2SiO_4 + 2CO_2 \uparrow \quad (2)$$

On the one hand, belite cements (BC) have two important assets, their low heat of hydration and their large amount of C-S-H after hydration, both yielding improved durability properties [11,12]. Moreover, other interesting properties related to the economy of a cement plant can be noted [13]: (i) the reduced LSF minimises the need for high quality limestone; (ii) the lower burning temperature results in a spare of fuel, and a reduction of the NO_x emissions; (iii) the expected increase in the costs of supplementary cementitious materials (SCMs), makes the use of Portland-like low heat clinker interesting for casting massive concrete; (iv) finally, they comply with existing standards, for instance, EN 197/1. On the other hand, the main barrier for BC usage is its slow hydration rate, not meeting current needs.

In a recently review, Cuesta et al. [11] summarizes the activation strategies for BCs as: (i) chemical activation by dopants at the clinkering stage, (ii) physical activation by fast cooling and intensive milling, i.e. inducing structural defects and larger surface area, and (iii) chemical activation at the hydration stage, for instance with accelerators like C-S-H seeding [14,15]. According to Chatterjee [16], many different oxides are effective as chemical activators, such as Ba, B, K, S, etc. More recent proposals are Fe_2O_3 [17] and boron [18]. A key chemical activation in BCs is the addition of calcium sulphate to the raw meal(s). Stanek and co-workers [10,19] have reported that the addition of about 5% SO_3 to the raw meals results in active belite clinkers developing early strength values comparable to those of PC. Calcium sulphate is preferable to other activators as it is safe and widely available. Cement notation will be followed hereafter.

Here, sulphur activated belite clinkers have been prepared by varying the amount of aluminium in the raw meals. It is known that aluminate phases in PC are partially responsible for the development of early strength, thus a possible strategy for accelerating strength development could be increasing the amount of these phases (mainly but not only C_3A) in the belite clinkers. However, it should be kept in mind that a high amount of soluble aluminate ions, at early hydration ages, can retard the calcium

silicate hydration, see for example [20–23]. An ordinary meal for Portland clinker production is characterized by a silica ratio (SR) in the range 2.0-3.0 and an alumina ratio (AR) between 1.0 and 4.0 [9]. Lower silica ratios (and higher alumina ratios) result in higher contents of interstitial phase(s), i.e. C_3A and C_4AF, that influence the hydration of the calcium silicate phases.

This study investigates the effect of the aluminium content on active belite clinkers reactivity by: i) keeping constant the LSF (i.e. not varying the C_3S/C_2S ratio); ii) keeping constant the SO_3 content (i.e. not changing the chemical belite activation); iii) maintaining fixed (and low) the Fe_2O_3 content of the raw meals; and iv) varying the silica/alumina ratio (i.e. SiO_2/Al_2O_3), in order to theoretically promote the formation of C_3A. This research shows that belite phase can reach a degree of reaction of 50% in one week under certain conditions.

2. Materials and Methods.

2.1. Materials and sample preparations.

Raw materials used for the preparation of the belite clinkers were all supplied by Buzzi Unicem: natural limestone and anhydrite are ordinarily used for industrial cement production; quartzite and bauxite are used as corrective in the raw meals for clinker production. Chemical composition of the raw materials is summarized in Table 1. The analyses were carried by dispersive X-ray Fluorescence (XRF), using a Panalytical Axios spectrometer on fused bead, prepared with a Breithländer autofluxer, 0.9 g of calcined sample plus Li-tethraborate in 1:10 dilution. The determination of the element content was performed with the IQ+ semi-quantitative software, and expressed as a percentage in weight of the corresponding metal oxides.

Table 1. Chemical composition of the raw materials (oxides, wt%).

	SiO_2	Al_2O_3	Fe_2O_3	CaO	MgO	SO_3	K_2O	TiO_2	LoI
Limestone	1.16	0.40	0.15	53.13	2.09	0.10	0.06	-	42.88
Quartzite	92.46	3.86	0.55	0.12	0.24	-	1.99	-	0.57
Anhydrite	0.75	0.53	0.21	38.50	0.05	48.55	-	-	10.55
Bauxite	10.10	58.20	1.10	-	-	-	-	2.10	16.00

Each material was separately milled in a vibrating mill, $d_{100} < 90$ µm. Raw meal mixtures were formulated by fixing the LSF value and decreasing the silica ratio by adding increasing amounts of bauxite. The resulting dosages of the three meals, labelled hereafter, Low-Al, Med-Al and High-Al, are summarized in Table 2. 1 wt% of calcium fluoride (commercial CaF_2 from Merck) was used as melting agent. Meals were granulated with a Heinrich granulator plate and dried at 105°C. Then, the burning step was performed using a Carbolite Bottom Loading Furnace model 16-3, at 1350°C for 30 minutes using a platinum crucible. After heating, the clinkers were rapidly cooled down under a flow of compressed air. The three studied compositions were prepared in large amounts, slightly larger than 1 kg, in order to have enough material to perform a compressive strength test according to EN 196-1.

Table 2. Composition of the raw meals and selected target values of LSF and SR.

	Low-Al	Med-Al	High-Al
LSF	83.0	83.0	83.0
SR	14.0	3.6	2.0
Limestone	74.2	71.4	68.8
Quartzite	18.0	15.4	13.0
Anhydrite	6.8	6.8	6.9
Bauxite	-	5.4	10.3
Fluorite	1.0	1.0	1.0

For the optical microscopy characterization, the clinkers were crushed in laboratory crusher and particles of selected sizes (between 3 and 5 mm) were embedded in resin, and shaped in form of cylinders (ø=20 mm; height=20 mm). One surface of the cylinders was smoothed and polished by employing a semi-automatic system (Struers Labosystem), using a sequence of MD-disks and clothes with diamond sprays for polishing. Specimens were etched with a 0.2% nitric acid solution in ethanol (Nital), immersing the polished surface for 10 seconds in the solution, and then washing it with isopropyl alcohol. Microscopic pictures were acquired with a metallographic microscope A1 Zeiss at different magnifications.

The clinkers were ground in a vibrating mill for 4 minutes. Particle size distributions of the three clinkers were measured on a Particle Size Analyzer Cilas model 920, and a summary of the results is given in Table 3. Ethanol was used as dispersing agent.

Table 3. Particle size distribution data for the investigated clinkers, determined from laser diffraction.

	Low-Al	Med-Al	High-Al
$D_{v,10}$ (μm)	0.75	0.79	0.78
$D_{v,50}$ (μm)	6.0	9.2	9.2
$D_{v,90}$ (μm)	36.4	40.0	71.4

2.2. Cement and paste preparations.

The cements were prepared by mixing the clinkers with anhydrite in a fixed mass ratio of 96:4. For the X-ray powder diffraction study, TiO_2 anatase 5.0 wt%, was added as internal standard to the dry cement prior to the water mixing. The internal standard approach allows to measure the total ACn (amorphous and crystalline non-determined) content as previously reported [24,25].

The pastes were prepared with a fixed water to cement (w/c) mass ratio of 0.50. They were mechanically mixed for 1 minute, then poured into individual plastic tubes and stored for different aging times: 1, 2, 7, 28 and 90 days. At a given time, the pastes were crushed in a jaw crusher at ~2 mm and placed in a desiccator under nitrogen. The samples within the desiccator were stored for 24 hours in an oven at 40°C in order to remove the unbound water.

2.3. Analytical techniques.

2.3.1. X-ray powder diffraction (XRPD). The XRPD data were collected by using a Bruker D4 Endeavor X-ray diffractometer working in Bragg-Brentano geometry. This equipment has a ceramic X-ray tube KFF ($CuK\alpha_{1,2}$ radiation) and a "Link Eye" detector. The key employed conditions were: a 2θ range of 8 to 50°; 0.02° of step size; and 0.5 s/step of counting time. For the clinkers, the patterns were acquired in pressed pellets prepared with an automatic pelletizer, Polab APM. For the pastes, the patterns were collected in powders, manual grinding in an agate motar, by front loading on PMMA rings with 25 mm well.

The Rietveld quantitative phase analysis (RQPA) was performed with the GSAS suite of programs and the EXPGUI graphic interface [26]. The optimized parameters were: background coefficients, zero-shift error, cell parameters, and peak shape parameters using a pseudo-Voigt function. The preferred orientation effect was observed for portlandite and monosulfate (AFm type phase) and it was corrected by the March-Dollase approach [27]. The employed crystal structures have been previously detailed [24,28,29].

2.3.2. Thermal analysis (TA). A TG/DSC 1 Mettler Toledo equipment was used for recording the thermal data of the pastes. Thermogravimetric data were collected on heating from 35 to 950 °C at 20 °C/min. Small fragments of a given paste were placed in 90 μl alumina crucible and 80 ml/min air flow was used. Data were processed using the StarE software of Mettler Toledo. The amount of free water (FW) was derived from the weight loss between 35 and 500 °C as given in equation (3) [30], where FW stands for free water; %W is the initial (nominal) water amount; Wl_{500} is the weight loss up to 500°C; and %C is the initial cement amount. It is acknowledged that C-S-H may release water

above 500ºC but it is overlapped with the weight loss of calcium carbonate, and therefore this (minor) amount is neglected here. Moreover, the chemically bound water contains the water in all hydrated phases: C-S-H, CH, AFt and monosulfate (AFm).

$$FW = \%W - Wl_{500} \times \frac{\%C}{100 - Wl_{500}} \quad (3)$$

2.3.3. Isothermal calorimetry. Heat flow measurements were performed for the pastes up to 12 days of hydration, at 20ºC, using a (TAM III – TA Instrument) isothermal calorimeter. 6 g of clinker/cement were weighed into a glass ampoule and the corresponding amount of water, w/c=0.50, was added. The mixing was performed externally (prior to the insertion of the ampoule in the chamber) using a small stirrer for 1 min. The flask was then sealed and placed into the calorimeter. The heat of hydration was determined by integration of the heat flow curve. The data for the first 40 minutes, after water mixing, were not taken as this time was needed for sample preparation and to reach thermal stability within the calorimeter.

2.3.4. Mortar measurements/tests.

Determination of flow of fresh mortars, w/c=0.50, was carried out following the procedure described in EN 1015-3, based on the measurement of the flow of a fresh mortar. A brief description is given here. A mortar is poured in a conic mould of 100 mm of base diameter and placed on a round jolting table with a flat surface. Then, the cone is lifted and the mortar is submitted to 15 jolts, flowing across the table. The diameter of the spread mortar is measured along two perpendicular directions. The low value is measured as, Flow (%) = $(L_s\text{-}L_0/L_0)\times100$, where L_s is the value of the diameter of the spread mortar after 15 jolts, and L_0 is the value of the initial diameter, in this case 100 mm.

For the determination of workability, the B method reported in EN 1015-9 was followed: the consistency value of the mortar was measured (as described in UNI EN 1015-3) after 10 minutes from the mixing and, subsequently, until the measured value differs 30 mm from the first measurement. Workability was expressed as the time (in minutes) required by the mortar to obtain a resistance to penetration of 0.5 N/mm^2 using a special apparatus as detailed in the standard.

For the determination of the compressive strengths, mortars were prepared and tested in accordance with EN 196–1. Prisms of dimensions 4×4×16 cm were cast using water, cement and sand in 0.5:1:3 mass ratio and stored for 24 h at 20°C and 95% RH in their moulds. After demoulding, they were cured in water until the compressive strength tests were performed at the desired ages (1, 7, 28 and 90 days). Three prisms were used for flexural data acquisition (not reported) and the six resulting specimens were employed for the compressive measurements. The reported data are the average of the six measurements.

Setting times were determined on cement pastes according to the EN 196-3 using a Vicat apparatus. The method requires a fresh cement paste characterised by a specific consistency which is poured in a conic mould and submitted to the penetration of a needle every minute. The initial setting time is the time (in minutes) required to have a distance of 6± 3 mm between the needle and the base of the paste. Similarly, the final setting time is the time required for the needle to penetrate less than 0.5 mm.

3. Results and discussion.

3.1. Clinker characterization. The chemical (from XRF) and mineralogical (from Rietveld analyses) compositions of the resulting clinkers are given in Tables 4 and 5, respectively.

Some observations can be extracted from the data reported in Table 5.

Firstly, and as designed, the main phase in the three clinkers is belite, always in amounts larger than 50 wt%. Minor element substitution invariably stabilizes the monoclinic, beta, phase. The unit cell volumes of β-belite were 346.8(1), 347.9(1) and 347.6(1) Å^3 for Low-Al, Med-Al and High-Al clinkers, respectively. A larger unit cell volume has been reported for belite activation [31–33], and

it is expected here because larger Al incorporation in belite yields bigger cells. Moreover, it was reported that SO_3 cement mineralization/activation took place at the calcium silicate phases mainly by the coupled substitution 3 $Si^{4+} \leftrightarrow S^{6+}$ + 2 Al^{3+} [34,35]. The molar SO_3 to alkali oxide ratio, R, should exceed 2 to get maximum substitution of sulfate within alite and belite. This is indeed the case in the clinkers prepared here, see Table 4. It is also worth noting that belite was reported to contain three times more sulfate than alite [34].

Table 4. Elemental analyses (wt% expressed as oxide contents, unless Fluor) for the three clinkers from XRF. R stands for the SO_3 to alkali oxide molar ratio.

	CaO	SiO_2	Al_2O_3	SO_3	Fe_2O_3	MgO	F	K_2O	Na_2O	TiO_2	Others	R
Low-Al	64.38	24.43	1.56	4.96	0.39	2.74	0.58	0.70	0.06	0.06	0.15	7.4
Med-Al	62.32	21.83	6.21	4.86	0.41	2.68	0.57	0.60	0.05	0.27	0.18	8.4
High-Al	60.55	19.70	10.32	4.74	0.51	2.34	0.58	0.51	0.05	0.52	0.17	9.7

Table 5. Mineralogical phase compositions for the three clinkers from Rietveld Quantitative Phase Analysis.*

	β-C_2S	C_3S-M3	o-C_3A	$C_{12}A_7$	$C_4A_3\bar{S}$	Fluorellesteadite	MgO	Dolomite
Low-Al#	58.2(3)	26.9(4)	-	-	0.4(1)	9.3(4)	2.4(1)	2.1(1)
Med-Al	55.6(3)	25.5(3)	0.8(1)	1.5(1)	5.6(1)	7.1(2)	2.5(1)	1.4(1)
High-Al	52.8(3)	22.3(3)	1.3(1)	4.1(2)	11.3(1)	4.7(1)	2.1(1)	1.2(1)

* The number in brackets are the standard deviations from the mathematical fits. The real errors could be larger mainly for the phases in low amounts. # This sample also contained 0.7(1) wt% of CaO.

Secondly, the three samples contained monoclinic alite, M3 polymorph, in amounts ranging 22-27 wt%. As expected, the amount of C_3S decreases along the three samples because there is less silicon in the meals. The alite unit cell volumes also evolve along the studied clinkers. The alite volumes were 4334(1), 4341(1) and 4344(1) $Å^3$ for Low-Al, Med-Al and High-Al clinkers, respectively. Larger values are likely due to higher Al^{3+} substitution within its crystal structure.

Thirdly, the increased amount of aluminium in the meals leads to the formation of ye'elimite and not of C_3A.

Fourthly, a high amount of sulfates was dosed in the clinker for chemically activating belite phase [10,19,35,36], see Table 4. Activation of belite was attempted through the possible solid solution, $Ca_2(Si_{1-3x}Al_{2x}S_xO_4)$ [34]. However, because the limited solubility of SO_4^{2-} anions within belite, there is an excess of sulfates which are fixed in other phases of the clinkers, mainly within crystalline ye'elimite, $Ca_4Al_6O_{12}(SO_4)$, and fluorellesteadite, $Ca_{10}(SiO_4)_3(SO_4)_3F_2$. This latter phase is formed because fluorite was used as mineralizer. It is possible to determine the amount of SO_3 in the clinker phases not bound to ye'elimite and fluorellesteadite from the data reported in Tables 4 and 5. The amount of SO_3 fixed in these two phases were 2.28, 2.44 and 2.61 wt% for Low-Al, Med-Al and High-Al clinkers, respectively. Therefore, the amount of SO_3 available to be incorporated mainly in the calcium silicate phases were 2.68, 2.42 and 2.13 wt%, respectively. This is expected to accelerate belite hydration rate.

Finally, and concerning the fluoride distribution, it should be noted that the reported amounts of fluorellesteadite in Table 4 account for 0.35, 0.27 and 0.18 wt% of F in Low-Al, Med-Al and High-Al clinkers, respectively. Therefore, 0.23, 0.30 and 0.40 wt% of F is incorporated in the typical clinkers phases mainly in alite as previously reported [34,37]. However, it should also be highlighted that large amounts of fluoride have been reported to delay alite hydration with the optimum content in PCs being close to 0.2-0.3 wt% of F [34,37,38]. Although fluorite was dosed in the same amount for the three clinkers, the different phase assemblages yielded a double of fluorides in the calcium silicate phases in High-Al when compared to Low-Al. This could have contributed to the delay in the

calcium silicate hydration rates for the cements with higher fluoride contents within the calcium silicate phases.

The clinkers were inspected by optical microscopy as described in the experimental section. The microscopy analysis of the three samples, see Fig. 1, reveals that both size and shape of belite crystals are quite similar. As expected, a higher amount of interstitial phases is observed in the High-Al clinker, see Fig. 1c.

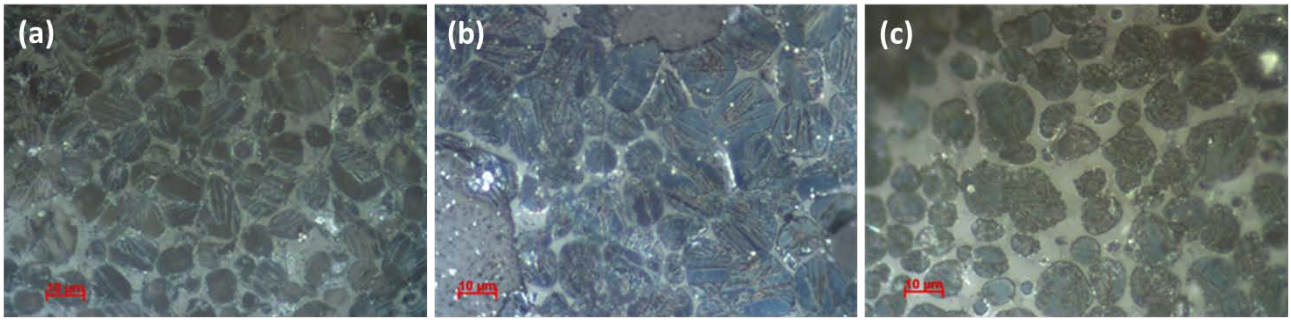

Fig. 1. Optical microphotographs for the three studied clinkers: (a) Low-Al, (b) Med-Al and (c) High-Al. 100× magnification.

3.2. Cement paste phase development by RQPA. The mineralogical phase analysis of the clinkers was reported above and now the discussion is centred in the hydration behaviour of the resulting cements. The raw powder diffraction patterns taken at 1, 2, 7, 28 and 90 days of hydration are shown in Fig. 2. Initially a qualitative analysis is carried out based on the observed diffraction peaks and their time evolution. Subsequently, a quantitative analysis of the degree of hydration (DoH) is carried out based on the RQPA results.

Concerning the sulphate-containing hydrated phases, the main observations are the following. For the Low-Al cement (SR 14) paste, the crystalline phase was just ettringite in minor amounts at all ages, see Fig. 2a. For the Med-Al cement (SR 3.6) paste, the first hydration products, i.e. at 1 day, were both AFt and monosulfate, the first being in higher amounts, see Fig. 2b. At seven days, the amount of AFt decreases leading to additional monosulfate formation. This behaviour is commonly observed when there is a lack of available sulfates and an excess of calcium aluminate(s), see for instance equation (4). For the High-Al cement (SR 2.0) paste, at 1 day both AFt and monosulfate phases are observed, but the second being in higher amounts, see Fig. 2c. AFt content decreases as hydration progresses and it fully disappears at 28 days reflecting the lack of sulfates for the relatively high amount of calcium aluminates.

$$Ca_6Al_2(OH)_{12}(SO_4)_3{\cdot}26H_2O\ (AFt) + 2\ Ca_3Al_2O_6 + 4\ H_2O \rightarrow 3\ Ca_4Al_2(OH)_{12}(SO_4){\cdot}6H_2O\ (AFm) \quad (4)$$

The crystallization, i.e. development, of portlandite is a good indicator for the C_3S hydration. Fig. 1a shows a large amount of crystalline $Ca(OH)_2$ (CH) at 1 day showing a high DoH of alite at this age. However, the analysis of portlandite content has to be done with care as it can be consumed by aluminate-rich clinker phases to yield monosulfoaluminate, see for instance equation (5) as an example for ye'elimite. It is acknowledged that there is no direct evidence of reaction (5) but there is a very important indirect observation. For Med-Al and High-Al pastes, the degree of reaction of alite can be higher than 50% and CH is not detected, see next. Therefore, it is concluded that for Med-Al and High-Al pastes at early ages, CH is being consumed in reactions like (5).

$$Ca_4Al_6O_{12}(SO_4) + 2\ CaSO_4 + 6\ Ca(OH)_2 + 30\ H_2O \rightarrow 3\ Ca_4Al_2(OH)_{12}(SO_4){\cdot}6H_2O\ (AFm) \quad (5)$$

For the quantitative analyses, the LXRPD data were treated by the Rietveld method as detailed in the experimental section. The RQPA results were normalized to 100 grams of pastes and they are given in the annex Tables A1 to A3. Based on these data, the phase evolutions for the three cement pastes are displayed in Fig. 3. The hydration behaviours of the three samples were quite different.

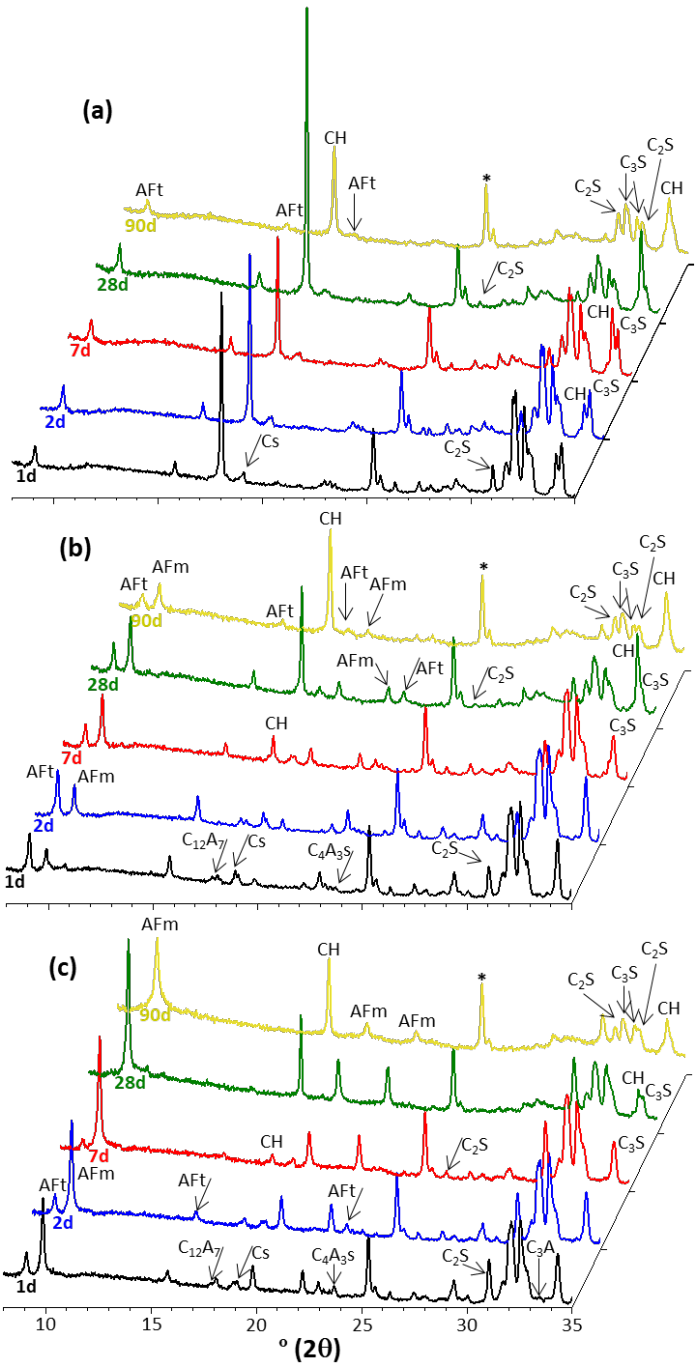

Fig. 2. Laboratory (CuK$\alpha_{1,2}$) powder diffraction patterns as function of hydration age for (a) Low-Al, (b) Med-Al and (c) High-Al pastes. The main peaks due to a given phase are labelled. The star denotes the main peak of the added internal standard, TiO_2-anatase.

The hydration behaviour of the silicate phases is noteworthy, see Fig. 3. For the Low-Al cement, C_3S shows a DoH of 89% already at 1 day and 91% at 7 days. Conversely, the DoH of alite for Med-Al was 61% and 91% at these hydration ages. Furthermore, this trend of lower reaction rate is even more conspicuous for High-Al cement. The DoH of alite was 54% and 84% at 1 and 7 days, respectively. For the three pastes at 28 days, the DoH for alite was invariably higher than 90%. Clearly, the presence of larger amounts of aluminates in the pore solution retards the hydration of alite at early ages as previously reported [20–23]. Portlandite phase evolution fully backs these findings although its presence has to be treated cautiously. After CH crystallization and if there is lack of sulfates, it can be consumed to yield monosulfate, as discussed just above. Reaction (5) contributes to explain the low measured amount of portlandite at 7 days in Med-Al and High-Al pastes in spite of a relatively large DoH for alite.

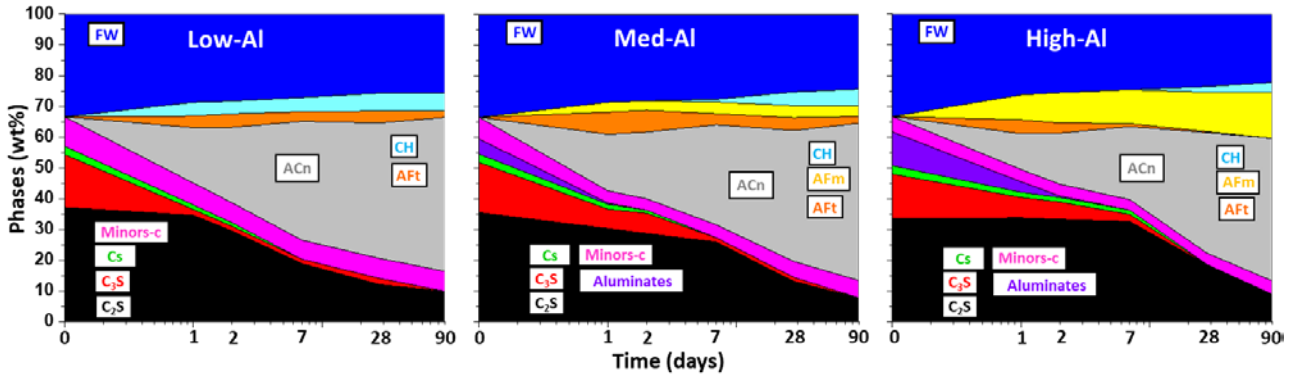

Fig. 3. Phase evolution for the three studied belite cement pastes, w/c=0.50, from RQPA and normalized to 100 grams of paste. The phases from bottom to top are: C_2S (black), C_3S (red), anhydrite (green), calcium aluminates (C_3A, $C_{12}A_7$ and $C_4A_3\bar{S}$ grouped together; purple) and Minors-cement (any other low reactivity (including fluorellesteadite; pink). The crystalline hydrated phases are: AFt (orange), monosulfate (AFm, yellow) and CH (light blue). Free water is given at the top, from the thermal study, as dark blue. The total amorphous content, ACn, determined by the internal standard methodology, and subtracting the free water in the calculations, is given as grey. This component includes mainly, but not only, C-S-H gel.

Concerning the DoH of the belite phase, its reaction rate is obviously slower than that of alite [11], but its trend along the studied cements is very informative. For Low-Al paste, the DoH of belite was 21, 49 and 73 % at 2, 7 and 28 days, respectively. It is very important to note that in the absence a significant amount of crystalline calcium aluminates, the reaction degree of belite phase at 7 days can be ~50%. This is explained by the activation of belite phase at the clinkering stage with sulfates. For Med-Al paste, the hydration rate of belite was slower, DOH being 20, 27 and 63% at the same ages, in spite of (i) the constant SO_3 content of the clinker, and (ii) having a larger unit cell volume. Both former points are consistent with belite activation, according to the current knowledge [11]. The value at 2 days seems to be anomalously high, likely due to the unavoidable experimental uncertainties. For High-Al paste, the DoH of belite is even slower: 0, 0 and 45%, 2, 7 and 28 days, respectively. There are two contributing factors that allow to justify a lower reaction rate of the calcium silicate phases in spite of the activation. Firstly, the fluoride content within this phase increase which is known to decrease their reaction rates [38]. Secondly, as the amount of anhydrite to formulate the cement was constant, more aluminates are available at early hydration age in Med-Al and High-Al samples. The presence higher amounts of aluminates in the pore solution at early time retards the hydration of alite [20–23]. The results presented in this work suggest that also soluble aluminates strongly influence, i.e. inhibits/delays, the hydration of belite at early ages, which should be taken into account for the future hydration acceleration of belite cements. Finally, at 90 days, the hydration degree of belite in the three cements ranges 75-80%. Therefore, at this late age, the influence of the aluminates in belite hydration is much less important.

3.3. Paste hydration by thermogravimetric analysis. The thermal traces for the investigated pastes hydrated for 1, 7, 28 and 90 days are shown in Fig. 4. A confirmation of the findings for the AFt and monosulfate behaviour, given earlier from the powder diffraction analyses, is derived here. Fig. 4(b) shows the endotherms mainly due to AFt and monosulfate, which are centred approximately at 120 and 200 ºC, respectively. The Low-Al pastes do not show a clear peak from monosulfate at any hydration age. For Med-Al pastes, the main peak at early ages is due to AFt, but the monosulfate peak is evident at all ages having the maximum integrated area at 28 days of hydration. For High-Al pastes, the peak due to AFt is present at early ages. However, the monosulfate peaks haver higher areas.

The portlandite contents, derived using the tangential method [39], also mirrors the data obtained from the XRPD study. For the Low-Al pastes, the CH content smoothly increases with hydration age unless for 90 days where a minor decrease is measured, likely due to carbonation (as the weight loss at 700 ºC increased). For the Med-Al pastes, the CH content is evident at 7 days and later ages and

increases smoothly. The absence of CH at 1 day, although C_3S has partly reacted, is in agreement with the RQPA results and justified by its consumption in reaction (5), given above. For the High-Al pastes, the CH content is evident only at 28 days and later. The absence of CH at 1 and 7 days, is again in agreement with the RQPA results and justified as previously detailed. The reduced amount of CH, mainly for High-Al, could decrease the carbonation resistance of the resulting binders. Finally, it is noteworthy that the amount of monosulfate seems to decrease at 90 days without the formation of any other crystalline phase. This behaviour is not fully understood and it deserves further investigations. However, it is noted that monosulfate diffraction peaks become broader at 90 days, see Fig. 2, and this microstructural change could have several origins.

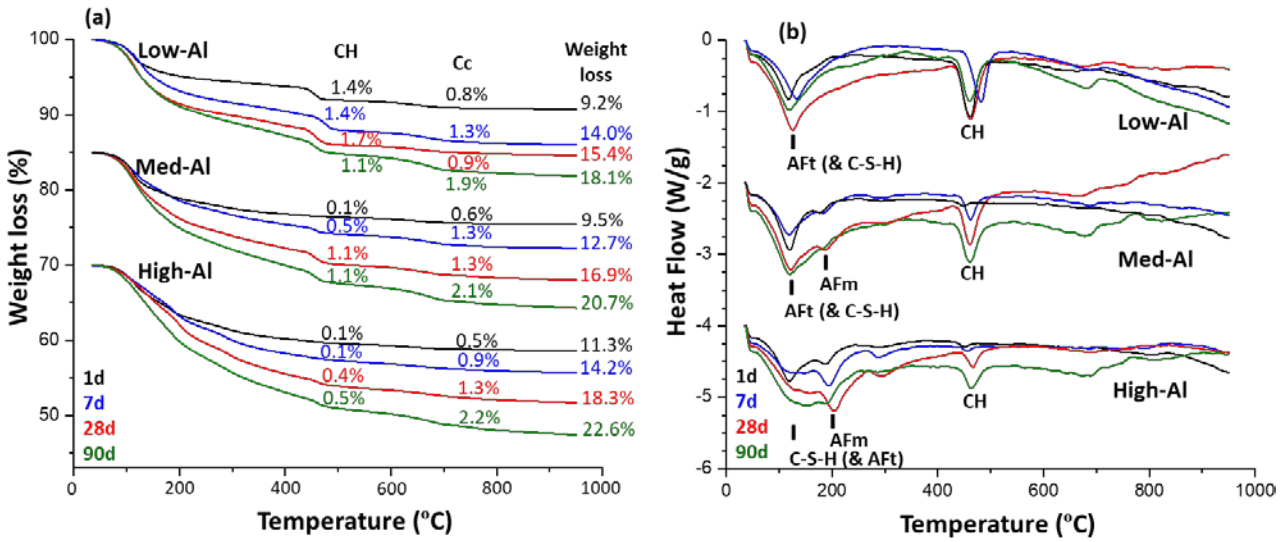

Fig. 4. Thermal analysis traces for the studied pastes at 1, 7, 28 and 90 days after arresting the hydrations. The curves for the Med-Al and High-Al series have been vertically displaced for clarity. However, the traces within a given series, i.e. just a function of the hydration time, are not displaced. (a) Thermogravimetric data. The derived portlandite and calcite contents (wt%) are given normalized to the neat pastes, i.e. containing the free water, for comparison to the RQPA results. (b) Differential thermal analysis data. The peaks corresponding to AFt, monosulfate and CH phases are labelled.

3.4. Early age hydration by isothermal calorimetry. Fig. 5 displays the isothermal calorimetric investigation, 20 ºC, for Low-Al and Med-Al pastes. Unfortunately, there was no remaining sample available for the measurement of High-Al. The heat flow curve for Low-Al clinker, without anhydrite addition (see Fig. 5a) shows a maximum at 12 hours of hydration. The dosage of 4 wt% of anhydrite barely affects the heat release pattern. The maximum for the cement took place at 13 hours. It is worth highlighting that SO_4^{2-} incorporation for this sample does not affect (accelerate) alite hydration because the aluminate amount in the clinker was very low, see Table 4. Therefore, C_3S hydration is assumed to be not retarded by the aluminates in pore solution, and anhydrite addition is not critical. However, this is not the case for Med-Al clinker. Without the addition of anhydrite, the maximum of heat release took place at ~100 hours, which was very likely due to alite hydration, see Fig. 5a. The addition of 4 wt% of anhydrite enormously accelerate alite hydration which now takes place at 22 hours of hydration. This behaviour is justified, because sulfate anions precipitate the aluminates in pore solution as ettringite (and also monosulfate, see previous sections) and therefore, aluminates in the pore solution retard much less alite hydration. Finally, it is noteworthy that for Med-Al clinker hydration, the heat release between 2 and 3 days was nearly zero, indicating almost no hydration reaction(s) during this period, in spite of its significant content of alite, ~15 wt% after the dilution with the water for the paste fabrication.

The cumulative heat released traces, for the four pastes, are displayed in Fig 5(b). The very early heat release patterns, in the two type of pastes, is different. Med-Al pastes (both clinker and cement) released more heat at very early ages, earlier than about 2 hours due to the hydration of the aluminates with the subsequent ettringite precipitation. This is not the case for Low-Al pastes where the heat

release at this age was much smaller, almost negligible, see inset in Fig. 5a. Finally, it is worth noting that for the studied pastes, the cumulative heats keep increasing after 6 days. This is likely due, at least partially, to the belite hydration, as also shown by RQPA.

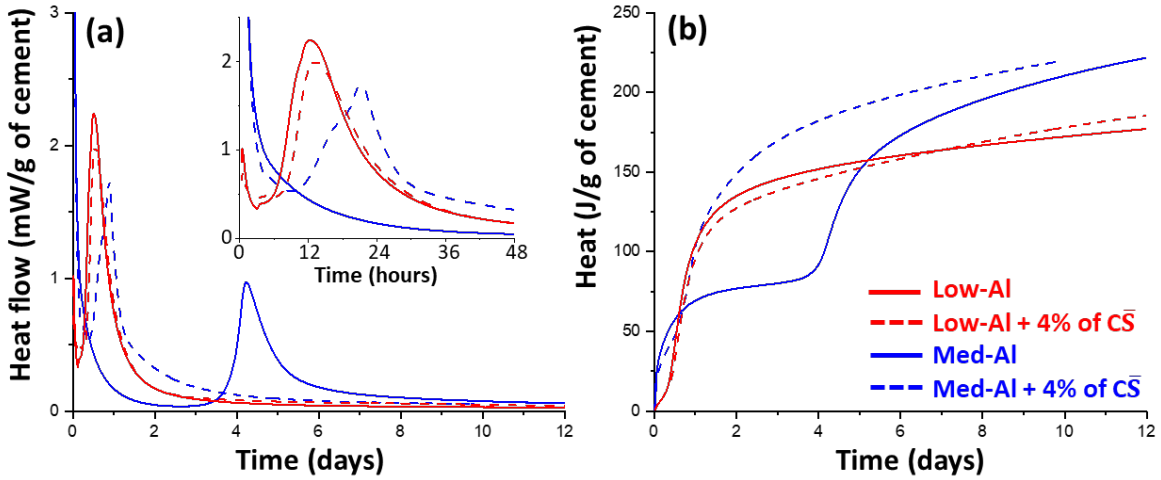

Fig. 5. Calorimetries for Low-Al and Med-Al pastes up to 12 days of hydration. (a) Heat flow curves (the inset displays the heat release in the first two days for better visualisation). (b) Cumulative heat released.

3.5. Mortar studies. The mortars were prepared as described in the experimental section and the key results are gathered in Table 6. For the studied belite cements, flowability and time of setting are strongly related to the amount of aluminium. Relatively high amounts of calcium aluminate phases ($C_4A_3\bar{S}$, $C_{12}A_7$ and C_3A) yielded less fluid mortars with faster setting for the employed amount of anhydrite, i.e. 4 wt%, which was kept constant for the three studied cements. The behaviour for High-Al clinker could be corrected with an optimization of the amount of sulphate carrier but the low amount of sample precluded this type of study. Conversely, the Low-Al cement had high flowability and long setting times indicating low reactivity at very early ages.

Table 6. Rheological and mechanical characterization results for the mortars prepared as described in the experimental section. The three cements contained 96 wt% of clinker and 4 wt% of anhydrite.

Test type	Low-Al (SR=14.0)	Med-Al (SR=3.6)	High-Al (SR=2.0)
Flow (%)	115	105	75
Workability (minutes)	160	30	3
Initial setting time (minutes)	250	50	6
Final setting time (minutes)	320	60	14
Compressive strengths at 1 d (MPa)[#]	3.4	3.6	6.3
Compressive strengths at 7 d (MPa)[$]	20	19	12
Compressive strengths at 28 d (MPa)[$]	38	36	25
Compressive strengths at 90 d (MPa)[$]	50	48	32

[#] All individual data at 1 d were within 2% of the corresponding average value.
[$] All individual data at 7 d, and later ages, were within 3.5% of the corresponding average value.

Concerning the mechanical strengths, they were relatively poor at 1 day, see Table 6. It should be noted that the low workability of High-Al cement did likely not allow to prepare a fully homogenous mortar within the moulds. Hence, the reported values of the compressive strength should be taken with care. For Low-Al cement, the low content of alite did not allow to obtain large value of compressive strength for the employed w/c ratio, 0.50. At seven days, where the DoH of belite is close to 50%, the compressive strength starts to rump up, being 20 MPa. Further hydration of belite for this cement led to 38 and 50 MPa at 28 and 90 days, respectively. The mechanical strength values of Med-Al cement did not vary much from those already discussed, see Table 6. It seems that the

positive effects from the calcium aluminate hydration are counterbalanced by the slower hydration rates of the calcium silicate phases.

4. Conclusions.

Belite clinkers with variable aluminium contents (Al_2O_3 percentage ranging from 1.5 to 10 wt%) were successfully burned with sulphur to stabilize and activate the belite phase. The average SO_3 content in the clinkers was 4.8 wt%. The total crystalline reactive calcium aluminate contents were 0.4, 7.9 and 16.7 wt% for Low-Al, Med-Al and High-Al clinkers, respectively.

Fluorite helps in the clinkering process, but resulted in inert fluorellesteadite, $Ca_{10}(SiO_4)_3(SO_4)_3F_2$, formation. This phase drained sulphates for AFt and monosulfate formation during hydration. Moreover, high amount of fluorides in calcium silicate phases for Med-Al and High-Al could contribute to hinder calcium silicate reactivities at early ages.

The reactivity of the resulting cement pastes, with a constant anhydrite content of 4.0 wt%, were studied by isothermal analysis, thermogravimetric characterisation and Rietveld quantitative phase analysis. It has been shown that calcium silicate hydration rates, both C_3S and C_2S, strongly depends on the aluminate available in pore solution. The degrees of hydration of alite at 1 day were approximately 89, 61 and 54% for Low-Al, Med-Al and High-Al cements, respectively. The degrees of reaction of belite at 7 days were close to 49, 27 and 0 % for Low-Al, Med-Al and High-Al cements, respectively. This clearly indicates the strong influence of aluminates in calcium silicate rates of hydration.

Chiefly, it is shown that belite phase can be activated at the clinkering stage with sulphur substitution (and likely also aluminium) leading to enhanced reactivity at relatively early ages. A β-belite degree of hydration close to 50 % at seven days is really noteworthy.

A clinker with low silica ratio value (SR=2.0, elemental Al_2O_3 content of 10.3 %) had a high content of calcium aluminates which resulted in poor flowability properties for the employed anhydrite amount of 4.0 %. Conversely, a clinker with high silica ratio value (SR=14.0, elemental Al_2O_3 content of 1.6 %) had very low content of calcium aluminates. In this case, the flowability was improved and setting time was larger indicating a very low reactivity at very early ages.

Finally, and comparing the early age mechanical properties of the belite cements with SR=14.0 and 3.6, the results indicate that the improvement from the reactivity of calcium aluminates in Med-Al are offset by the lower reactivity of the silicate phases. The retarding effect of aluminates on the calcium silicate hydration rates is firmly established. Hence, further investigations are required for the relatively low aluminate content region, SR ranging 10-5, with the aim of retaining high calcium silicate reactivity with a sufficiently high ettringite content. This combination should yield larger mechanical strengths at early ages which would remove the main limitation of belite cements.

CRediT authorship contribution statement.

C.R.-S.: methodology, investigation, data curation, writing–original draft, review & editing. **D. G.**: conceptualization, supervision, methodology, investigation, data curation, writing–original draft, review & editing. **S.I.**: investigation, review & editing. **F.C.**: investigation, review & editing. **M.A.G.A.**: supervision, investigation, writing–original draft, review & editing.

Acknowledgement. The research carried out in Malaga was supported by PID2020-114650RB-I00 research grant from the Spanish Government, which is co-funded by ERDF.

Declaration of competing interest. The authors declare that they have no known competing financial interests or personal relationships that could have appeared to influence the work reported here.

Data availability. Raw data are available from the corresponding authors upon request.

5. Annex. Rietveld quantitative phase analysis results for the three series are given in Tables A1-A3.

Table A1. Rietveld quantitative phase analysis output for the Low-Al (SR=14.0) series.

	t_0	1 d	2 d	7 d	28 d	90 d
C_3S-M3	17.2	1.9(3)	1.5(3)	1.4(4)	2.0(5)	-
β-C_2S	37.2	34.6(2)	29.5(2)	18.9(3)	12.1(5)	9.9(5)
$C\bar{S}$	2.7	1.5(2)	1.2(2)	-	-	-
MgO	1.5	1.5(2)	1.3(1)	1.2(2)	1.1(3)	1.0(3)
Dolomite	1.3	-	-	-	-	-
F-ellestadite	6.0	5.6(3)	5.2(3)	5.0(4)	5.4(6)	5.5(5)
CaO	0.4	-	-	-	-	-
$C_4A_3\bar{S}$	0.3	-	-	-	-	-
CH	0.00	4.4(1)	4.1(1)	4.6(1)	5.8(2)	6.0(2)
AFt	0.00	3.8(3)	4.4(3)	3.2(4)	3.9(5)	2.1(5)
FW	33.33	28.8	28.2	27.1	25.7	25.7
ACn	0.00	18.0	24.5	38.6	44.0	50.0

Table A2. Rietveld quantitative phase analysis output for the Med-Al (SR=3.6) series.

	t_0	1 d	2 d	7 d	28 d	90 d
C_3S-M3	16.3	6.3(3)	6.6(3)	1.4(3)	1.3(5)	-
β-C_2S	35.6	30.4(3)	28.8(3)	26.0(2)	13.2(5)	7.8(6)
o-C_3A	0.5	-	-	-	-	-
$C_{12}A_7$	1.0	-	-	-	-	-
$C_4A_3\bar{S}$	3.6	0.4(1)	-	-	-	-
$C\bar{S}$	2.7	1.6(2)	1.0(2)	-	-	-
MgO	1.6	1.2(1)	1.3(2)	1.3(1)	1.3(2)	1.3(2)
Dolomite	0.9	-	-	-	-	-
F-ellestadite	4.5	2.8(3)	2.4(2)	2.9(2)	3.9(5)	4.4(6)
AFt		7.2(3)	7.1(3)	3.6(2)	4.2(5)	2.2(5)
CH		-	-	0.9(1)	4.5(2)	5.6(2)
AFm-$C_4A_2\bar{S}H_{12}$		3.2(3)	3.1(1)	3.8(2)	3.9(5)	3.3(8)
FW	33.33	28.2	28.1	27.6	25.1	24.2
ACn	0.00	18.4	21.7	32.6	42.6	51.2

Table A3. Rietveld quantitative phase analysis output for the High-Al (SR=2.0) series.

	t_0	1 d	2 d	7 d	28 d	90 d
C_3S-M3	14.5	6.6(2)	5.6(2)	2.3(2)	-	-
β-C_2S	33.5	33.8(3)	33.3(3)	32.6(2)	18.6(5)	8.9(8)
o-C_3A	1.0	1.2(1)	-	-	-	-
$C_{12}A_7$	2.6	1.0(1)	-	-	-	-
$C_4A_3\bar{S}$	7.4	1.2(1)	0.5(1)	-	-	-
$C\bar{S}$	2.7	1.7(2)	1.5(1)	1.4(1)	-	-
MgO	1.4	1.6(1)	1.6(1)	1.4(1)	1.2(2)	1.2(2)
Dolomite	0.7	0.5(2)	0.5(1)	-	-	-
F-ellestadite	2.9	1.9(3)	1.7(3)	2.0(2)	2.5(2)	3.2(7)
AFt		4.5(2)	3.3(2)	1.0(2)	0.3(2)	-
CH		-	-	-	1.8(2)	3.2(7)
AFm-$C_4A_2\bar{S}H_{12}$		8.1(2)	9.9(3)	11.0(4)	12.8(4)	15.0(7)
FW	33.33	26.4	25.5	24.7	23.5	21.8
ACn	0.00	11.6	16.6	23.7	39.2	46.3

References

[1] International Energy Agency, IEA; Cement Sustainability Initiative, CSI; World Business Council for Sustainable Development, WBCSD, Technology Roadmap Low-Carbon Transition in the Cement Industry, 2018. https://www.iea.org/reports/technology-roadmap-low-carbon-transition-in-the-cement-industry.

[2] E. Gartner, Industrially interesting approaches to “low-CO2” cements, Cem. Concr. Res. 34 (2004) 1489–1498. https://doi.org/10.1016/J.CEMCONRES.2004.01.021.

[3] E. Gartner, H. Hirao, A review of alternative approaches to the reduction of CO2 emissions associated with the manufacture of the binder phase in concrete, Cem. Concr. Res. 78 (2015) 126–142. https://doi.org/10.1016/J.CEMCONRES.2015.04.012.

[4] E. Gartner, T. Sui, Alternative cement clinkers, Cem. Concr. Res. (2017). https://doi.org/10.1016/j.cemconres.2017.02.002.

[5] M.A.G. Aranda, A.G. De la Torre, Sulfoaluminate cement, in: F. Pacheco-Torgal, S. Jalali, J. Labrincha (Eds.), Eco-Efficient Concr., 2013: pp. 488–522. https://doi.org/10.1533/9780857098993.4.488.

[6] R.S. Anderson, S.P. Anderson, Geomorphology: The Mechanics and Chemistry of Landscapes., Cambridge University Press, 2010.

[7] C.D. Lawrence, The Production of Low-Energy Cements, in: P.C. Hewlett (Ed.), Lea’s Chem. Cem. Concr., 4th editio, Elsevier, 2004: pp. 436–470.

[8] L. Wang, H.Q. Yang, S.H. Zhou, E. Chen, S.W. Tang, Mechanical properties, long-term hydration heat, shinkage behavior and crack resistance of dam concrete designed with low heat Portland (LHP) cement and fly ash, Constr. Build. Mater. 187 (2018) 1073–1091. https://doi.org/10.1016/J.CONBUILDMAT.2018.08.056.

[9] H.F.W. Taylor, Cement chemistry. 2nd ed., Acad. Press. 20 (1997) 335. https://doi.org/10.1016/S0958-9465(98)00023-7.

[10] T. Staněk, P. Sulovský, Active low-energy belite cement, Cem. Concr. Res. 68 (2015) 203–210. https://doi.org/10.1016/J.CEMCONRES.2014.11.004.

[11] A. Cuesta, A. Ayuela, M.A.G. Aranda, Belite cements and their activation, Cem. Concr. Res. 140 (2021) 106319. https://doi.org/10.1016/j.cemconres.2020.106319.

[12] S. Irico, S. Mutke, F. Bertola, D. Gastaldi, L. Capelli, F. Canonico, Durability of high belite cement as new technical solution for concrete, in: Acta Polytech. CTU Proc. Vol 33, 2022: pp. 245–249. https://doi.org/https://doi.org/10.14311/APP.2022.33.0245.

[13] F. Canonico, Special binders as an alternative to Portland cement, in: 20th Int. Conf. Build. Mater., Weimar, 2015: pp. 410–422.

[14] A. Morales-Cantero, A. Cuesta, A.G. De la Torre, I. Santacruz, O. Mazanec, P. Borralleras, K.S. Weldert, D. Gastaldi, F. Canonico, M.A.G. Aranda, C-S-H seeding activation of Portland and Belite Cements: an enlightening in situ synchrotron powder diffraction study, Cem. Concr. Res. 161 (2022) 106946. https://doi.org/10.1016/j.cemconres.2022.106946.

[15] A. Morales-Cantero, A. Cuesta, A.G.D. la Torre, O. Mazanec, P. Borralleras, K.S. Weldert, D. Gastaldi, F. Canonico, M.A.G. Aranda, Portland and Belite Cement Hydration Acceleration by C-S-H Seeds with Variable w/c Ratios, Materials (Basel). 15 (2022) 3553. https://doi.org/10.3390/MA15103553.

[16] A.K. Chatterjee, High belite cements—Present status and future technological options: Part I, Cem. Concr. Res. 26 (1996) 1213–1225. https://doi.org/10.1016/0008-8846(96)00099-3.

[17] L. Kacimi, A. Simon-Masseron, S. Salem, A. Ghomari, Z. Derriche, Synthesis of belite

cement clinker of high hydraulic reactivity, Cem. Concr. Res. 39 (2009) 559–565. https://doi.org/10.1016/j.cemconres.2009.02.004.

[18] D. Koumpouri, G.N. Angelopoulos, Effect of boron waste and boric acid addition on the production of low energy belite cement, Cem. Concr. Compos. 68 (2016) 1–8. https://doi.org/10.1016/j.cemconcomp.2015.12.009.

[19] M. Boháč, D. Kubátová, M. Krejčí Kotlánová, I. Khongová, A. Zezulová, R. Novotný, M.T. Palou, T. Staněk, D. Všianský, The role of Li2O, MgO and CuO on SO3 activated clinkers, Cem. Concr. Res. 152 (2022) 106672. https://doi.org/10.1016/j.cemconres.2021.106672.

[20] L. Nicoleau, E. Schreiner, A. Nonat, Ion-specific effects influencing the dissolution of tricalcium silicate, Cem. Concr. Res. 59 (2014) 118–138. https://doi.org/10.1016/j.cemconres.2014.02.006.

[21] E. Pustovgar, R.K. Mishra, M. Palacios, J.-B. d'Espinose de Lacaillerie, T. Matschei, A.S. Andreev, H. Heinz, R. Verel, R.J. Flatt, Influence of aluminates on the hydration kinetics of tricalcium silicate, Cem. Concr. Res. 100 (2017) 245–262. https://doi.org/10.1016/j.cemconres.2017.06.006.

[22] D. Wagner, F. Bellmann, J. Neubauer, Influence of aluminium on the hydration of triclinic C3S with addition of KOH solution, Cem. Concr. Res. 137 (2020) 106198. https://doi.org/10.1016/j.cemconres.2020.106198.

[23] T. Hirsch, Z. Lu, D. Stephan, Effect of different sulphate carriers on Portland cement hydration in the presence of triethanolamine, Constr. Build. Mater. 294 (2021) 123528. https://doi.org/10.1016/j.conbuildmat.2021.123528.

[24] M.A.G. Aranda, A.G. De la Torre, L. Leon-Reina, Rietveld Quantitative Phase Analysis of OPC Clinkers, Cements and Hydration Products, Rev. Mineral. Geochemistry. 74 (2012) 169–209. https://doi.org/10.2138/rmg.2012.74.5.

[25] A.G. De la Torre, S. Bruque, M.A.G. Aranda, Rietveld quantitative amorphous content analysis, J. Appl. Crystallogr. 34 (2001) 196–202. https://doi.org/10.1107/S0021889801002485.

[26] A.C. Larson, R.B. Von Dreele, General structure analysis system (GSAS), Los Alamos Natl. Lab. Rep. LAUR. 748 (2004) 86–748.

[27] W.A. Dollase, Correction of intensities of preferred orientation in powder diffractometry: application of the march model, J. Appl. Crystallogr. 19 (1986) 267–272. https://doi.org/10.1107/S0021889886089458.

[28] M.A.G. Aranda, A. Cuesta, A.G. De la Torre, I. Santacruz, L. León-Reina, Diffraction and crystallography applied to hydrating cements, in: H. Pöllmann (Ed.), Cem. Mater. Compos. Prop. Appl., De Gruyter, Berlin, Boston, Germany, 2017: pp. 31–60. https://doi.org/10.1515/9783110473728-003.

[29] A.G. De la Torre, I. Santacruz, A. Cuesta, L. León-Reina, M.A.G. Aranda, Diffraction and crystallography applied to anhydrous cements, in: H. Pöllmann (Ed.), Cem. Mater., De Gruyter, 2017: pp. 3–29.

[30] J.D. Zea-Garcia, A.G. De la Torre, M.A.G. Aranda, I. Santacruz, Processing and characterisation of standard and doped alite-belite-ye'elimite ecocement pastes and mortars, Cem. Concr. Res. 127 (2020) 105911. https://doi.org/10.1016/j.cemconres.2019.105911.

[31] K. Morsli, A.G. De la Torre, M. Zahir, M.A.G. Aranda, Mineralogical phase analysis of alkali and sulfate bearing belite rich laboratory clinkers, Cem. Concr. Res. 37 (2007) 639–646. https://doi.org/10.1016/j.cemconres.2007.01.012.

[32] K. Morsli, A.G. De la Torre, S. Stöber, A.J.M. Cuberos, M. Zahir, M.A.G. Aranda,

Quantitative phase analysis of laboratory-active belite clinkers by synchrotron powder diffraction, J. Am. Ceram. Soc. 90 (2007) 3205–3212. https://doi.org/https://doi.org/10.1111/j.1551-2916.2007.01870.x.

[33] M. Yamashita, H. Tanaka, E. Sakai, K. Tsuchiya, Mineralogical study of high SO3 clinker produced using waste gypsum board in a cement kiln, Constr. Build. Mater. 217 (2019) 507–517. https://doi.org/10.1016/j.conbuildmat.2019.05.098.

[34] A. Emanuelson, A.R. Landa-Cánovas, S. Hansen, A comparative study of ordinary and mineralised Portland cement clinker from two different production units Part II: Characteristics of the calcium silicates, Cem. Concr. Res. 33 (2003) 1623–1630. https://doi.org/10.1016/S0008-8846(03)00114-5.

[35] Z. Yang, X. Tao, G. Wang, W. Li, Study on Preparation of Low Heat High Belite Clinker from Waste Mortar and Its Modification, Materials (Basel). 15 (2022) 3196. https://doi.org/10.3390/ma15093196.

[36] V. Isteri, K. Ohenoja, T. Hanein, H. Kinoshita, H. Kletti, C. Rößler, P. Tanskanen, M. Illikainen, T. Fabritius, Ferritic calcium sulfoaluminate belite cement from metallurgical industry residues and phosphogypsum: Clinker production, scale-up, and microstructural characterisation, Cem. Concr. Res. 154 (2022) 106715. https://doi.org/10.1016/j.cemconres.2022.106715.

[37] A. Emanuelson, S. Hansen, E. Viggh, A comparative study of ordinary and mineralised Portland cement clinker from two different production units: Part I: Composition and hydration of the clinkers, Cem. Concr. Res. 33 (2003) 1613–1621. https://doi.org/10.1016/S0008-8846(03)00115-7.

[38] G.. Moir, F.P. Glasser, Mineralisers, modifiers and activators in the clinkering process, in: Proc. 9th Int. Congr. Chem. Cem. New Delhi, Vol. 1, Natl. Counc. Cem. Build. Mater. New Delhi, 1992: pp. 125– 152.

[39] K.L. Scrivener, R. Snellings, B. Lothenbach, A Practical Guide to Microstructural Analysis of Cementitious Materials, CRC Press, Boca Raton, FL, 2016.